



HAL
open science

Enhancement of photocurrent in epitaxial lift-off thin-film GaInNAsSb solar cells due to light-confinement structure

Naoya Miyashita, Benoît Behaghel, Jean-Francois Guillemoles, Yoshitaka Okada

► To cite this version:

Naoya Miyashita, Benoît Behaghel, Jean-Francois Guillemoles, Yoshitaka Okada. Enhancement of photocurrent in epitaxial lift-off thin-film GaInNAsSb solar cells due to light-confinement structure. Applied Physics Express, 2018, 11 (7), pp.072301. 10.7567/apex.11.072301 . hal-01972796

HAL Id: hal-01972796

<https://hal.science/hal-01972796>

Submitted on 15 Jan 2019

HAL is a multi-disciplinary open access archive for the deposit and dissemination of scientific research documents, whether they are published or not. The documents may come from teaching and research institutions in France or abroad, or from public or private research centers.

L'archive ouverte pluridisciplinaire **HAL**, est destinée au dépôt et à la diffusion de documents scientifiques de niveau recherche, publiés ou non, émanant des établissements d'enseignement et de recherche français ou étrangers, des laboratoires publics ou privés.

LETTERS

Enhancement of photocurrent in epitaxial lift-off thin-film GaInNAsSb solar cells due to light-confinement structure

To cite this article: Naoya Miyashita *et al* 2018 *Appl. Phys. Express* **11** 072301

View the [article online](#) for updates and enhancements.



Enhancement of photocurrent in epitaxial lift-off thin-film GaInNAsSb solar cells due to light-confinement structure

Naoya Miyashita^{1,2*}, Benoît Behaghel^{2,3}, Jean-François Guillemoles^{2,3}, and Yoshitaka Okada^{1,2}

¹Research Center for Advanced Science and Technology (RCAST), The University of Tokyo, Meguro, Tokyo 153-8904, Japan

²LIA-NextPV, RCAST and CNRS, The University of Tokyo, Meguro, Tokyo 153-8904, Japan

³IRDEP, site EDF R&D, 6 quai Watier, 78400 Chatou, France

*E-mail: miyashita@mbe.rcast.u-tokyo.ac.jp

Received May 11, 2018; accepted May 28, 2018; published online June 8, 2018

This work focuses on the characterization of GaInNAsSb solar cells whose substrates are removed via the epitaxial lift-off (ELO) technique. As a result of the substrate removal, increases in the photocurrent and the interference feature were clearly observed. This is clear evidence of the light-confinement effect, whereby some of the unabsorbed photons at the rear metal contact were reflected back towards the front side of the ELO thin-film cell. We successfully demonstrated that the ELO technique can be applied for the GaInNAsSb cell, and the light management should add flexibility in designing the cell structures. © 2018 The Japan Society of Applied Physics

Recently, the epitaxial lift-off (ELO) technique, which allows the separation of the epitaxial layer from its substrate, has attracted considerable interest owing to its large potential for the cost reduction of III–V solar cells and optoelectronic devices.^{1–3} In the ELO concept, the separation of the epitaxial layer is based on the difference in the etching rates between a preinserted release layer and the neighboring layer materials. One of the most common combinations for ELO in GaAs-based devices is $\text{Al}_x\text{Ga}_{1-x}\text{As}$ and hydrogen fluoride (HF) as the release layer and the etchant, respectively, where the etching selectivity of the HF in the $\text{Al}_x\text{Ga}_{1-x}\text{As}$ ($x > 0.7$) to the GaAs is on the order of 10^5 – 10^6 .⁴ By using this concept, the separated substrates can be reused multiple times, and the proportion of the substrate cost to the total solar-cell production cost is reduced.^{5,6} On the other hand, the released standalone device layer opens up novel applications, such as flexible and lightweight solar cells. Furthermore, in III–V ELO thin-film solar cells, high conversion efficiencies have been reported,^{7,8} which are due in part to the efficient photon-recycling effect.⁹ In the thin-film solar cells, several approaches for optical management can be applied to enhance the light absorption, e.g., increasing the optical path length (OPL) with a light-scattering back pattern^{10,11} or using Fabry–Pérot (FP) cavity resonances.¹² These approaches are particularly effective for multi-quantum well^{13–16} and quantum-dot^{17–19} solar cells whose optical thickness is often limited owing to the growth constraints.^{16–18}

Dilute nitrides, which are promising for future multijunction solar cells (MJSCs),²⁰ face similar difficulties. In general, it is not easy to extract a sufficient photocurrent in the dilute-nitride cell, because of its poor minority-carrier properties;²¹ hence, dilute nitrides require built-in field-assisted carrier collection to extract photocarriers.^{20,22} Considering the GaInP/GaAs/GaInNAsSb triple-junction configuration, both a GaInNAsSb absorber thickness of $>2\ \mu\text{m}$ and a wide built-in field are important for current matching among the subcells.²² On the other hand, by utilizing light management, a sufficient photocurrent can be achieved in a thinner GaInNAsSb subcell. In this study, we applied the ELO technique to dilute-nitride GaInNAsSb solar cells and demonstrated the enhancement of the photocurrent due to the light-confinement effect by releasing the device thin film from its substrate.

The GaInNAsSb solar-cell samples used in this study were grown on GaAs substrates via radiofrequency plasma-assisted

Table I. Structure of the present ELO thin-film GaInNAsSb solar cell. The thickness values were obtained from the fitting.

Layer	Thickness (μm)
n^+ -GaAs	0.100
n -AlGaAs	0.0273
n -GaAs	0.182
i -GaInNAsSb	0.912
p -GaAs	0.456
p -AlGaAs	0.0912
p^+ -GaAs	0.456

molecular beam epitaxy (MBE). As shown in Table I, the device for the ELO process consists of an n^+ -GaAs contact, an n - $\text{Al}_{0.5}\text{Ga}_{0.5}\text{As}$ window, an n -GaAs/ i -GaInNAsSb/ p -GaAs double heterojunction, a p - $\text{Al}_{0.5}\text{Ga}_{0.5}\text{As}$ back surface field, and p^+ -GaAs contact layers. This n - i - p structure was grown inverted on an AlAs layer with 20-nm thickness, which was inserted as a release layer in the ELO process. As a reference device, the same n - i - p double heterojunction structure grown upright on the p -GaAs substrate was characterized with its substrate. The front contact metal consisted of AuGe/Au for both devices, whereas the rear contact metal was Au for the thin-film cell and In for the reference cell. No antireflection coating (ARC) was utilized.

Before the ELO process, a Au metal layer was deposited onto the top surface of the inverted sample. This Au layer was utilized for both the back reflector and the contact metal. We employed the weight-assisted ELO (W-ELO) method³ for separating the device thin film from its substrate. For this purpose, the sample was attached to a flexible handling substrate (polyethylene terephthalate film) and a support rod, as shown in Fig. 1. The ELO was conducted for the $11 \times 11\ \text{mm}^2$ chip sample using 12% HF and a process temperature of $\sim 25\ ^\circ\text{C}$. The device film was successfully separated after $\sim 7\ \text{h}$, and no apparent crack was generated. Then, the patterned front contact metal of AuGe/Au was formed. Finally, mesa pattern etching was performed to define the device area and expose the rear-side metal contact.

Figure 2 compares the ELO thin-film GaInNAsSb cell with a reference GaInNAsSb cell having a rigid GaAs substrate, with regard to the current density–voltage (J - V) and the external quantum efficiency (EQE) characteristics. These measure-

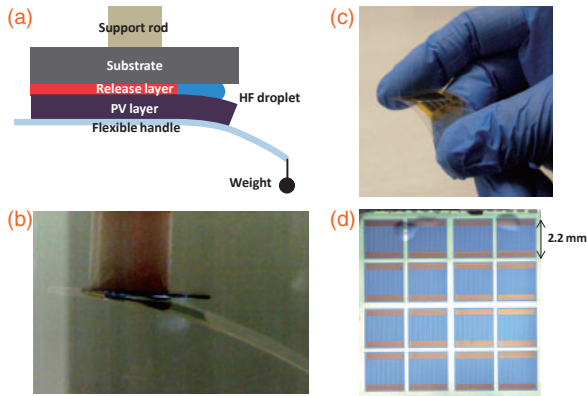


Fig. 1. (a) Schematic of the W-ELO setting and snapshots of (b) the W-ELO process and (c, d) the fabricated ELO thin-film cells.

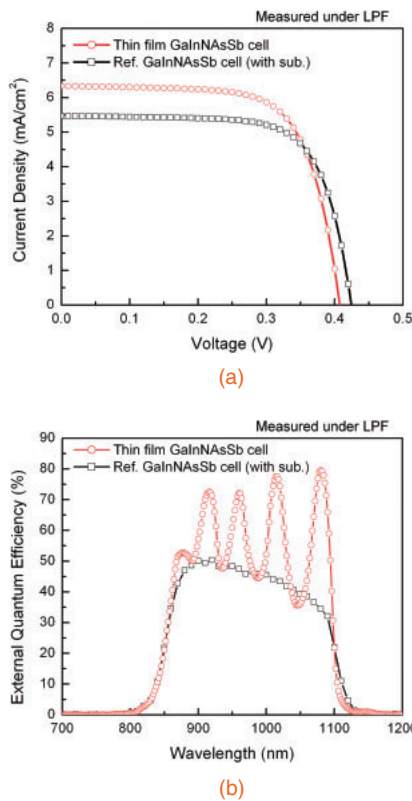


Fig. 2. (a) Light J - V curves and (b) EQE spectra of the ELO thin-film cell and the reference cell measured under an LPF.

ments were performed under each light source through a long-pass filter (LPF). We used a filter with a cut-off wavelength of 860 nm, which nearly matches the GaAs absorption edge, to simulate the performance of the GaInNAsSb subcell beneath the GaAs filtering in the triple-junction configuration. In this situation, the >870 -nm light can be absorbed only by the GaInNAsSb layer for the present devices. Regarding the J - V characteristics, compared with the reference device, a higher short-circuit current density (J_{SC}) was observed for the thin-film cell. The filtered EQE spectra more clearly indicate the increase in the photocurrent in most of the wavelength range, and the resonance feature also appears. This is because the present ELO thin-film cell structure plays the role of an FP cavity, where the light absorption can be increased through multiple roundtrips between the front side and the rear Au

Table II. Summary of the J_{SC} , V_{OC} , and FF values for filtered light J - V curves of the ELO thin-film and reference cells.

	J_{SC} (mA/cm ²)	V_{OC} (V)	FF (%)
Thin film cell	6.33	0.408	0.694
Reference cell	5.46	0.424	0.711

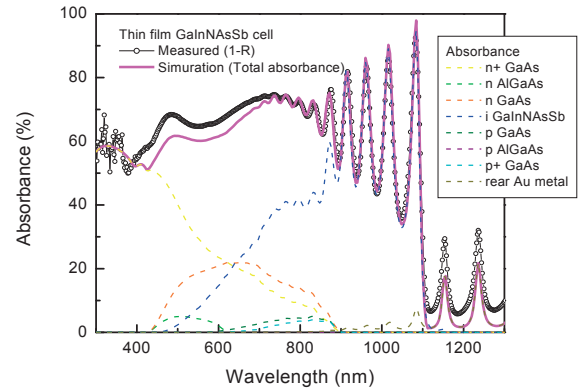


Fig. 3. Measured and calculated absorption spectra of the ELO thin-film GaInNAsSb cell.

reflector. Regarding the >870 nm photons, the ~ 1.0 - μm GaInNAsSb layer is not thick enough for full absorption. This situation provides another chance for such transmitted photons to be absorbed in the GaInNAsSb layer, resulting in an overall reduction of the transmission loss and hence an increase of the photocurrent. On the other hand, comparable open-circuit voltage (V_{OC}) and fill factor (FF) values were obtained between the two devices, as summarized in Table II. The slightly lower V_{OC} and FF for the thin-film cell might be due to the non-ideal ohmic contact at the back side. From the J - V curves in the high-current range of -100 to -200 mA/cm² in the positive-bias region, we extracted the series-resistance values for both devices: 0.82 and $0.46 \Omega \text{ cm}^2$ for the thin-film and reference cells, respectively. We consider that the larger series resistance in the thin-film cell contributed to the slightly lower V_{OC} and FF.

Next, we measured the absorbance spectrum (in black line) of the thin-film cell, as shown in Fig. 3. The absorbance, A , was obtained as $A = 1 - R$, where R represents the measured reflectance at the front surface of the present thin-film device. A clear FP resonance feature is observed in the long-wavelength region above ~ 700 nm, which is due to the interference between the back and front interfaces, creating an FP cavity in the device structure. The FP effect was simulated using a transfer-matrix model, which considers multiple reflections of the incident light in the layer stack of the device and allows us to calculate the absorbance in each layer. The measured absorbance spectrum was used to fit the total thickness of the FP cavity. For the calculation, first, ellipsometry analysis for a separated grown GaInNAsSb film sample was performed to extract the refractive (n) and extinction (k) indices. The effect of the Urbach tail is commonly observed in compound materials,^{23–25} and fitting with the unfiltered EQE spectrum shows that it cannot be neglected in the calculation. However, the feature of the Urbach tail was not apparent in the extracted k spectrum, which is because the resolution of lower limit in our ellipsometry measurement

was not high enough. Hence, the Urbach tail was complemented by the analysis of the near-bandedge feature of the EQE spectrum of the identical device. The typical exponential behavior of the tail of the absorption-coefficient spectrum for the photon energy, E , is given by²³⁾

$$\alpha(E) = \alpha_0 \exp\left(\frac{E - E_g}{E_0}\right), \quad (1)$$

where we treat α_0 and E_0 as the fitting parameters. Physically, E_0 represents the width of the tail. The E_0 for our GaInNAsSb film was deduced to be 10.5 meV. We consider that the fitting was reasonable because the typical value of E_0 for the GaAs is approximately 10 meV.^{23,24)} As the fitting parameter, a coefficient representing the thickness ratio was chosen to correct the difference between the designed and actual epitaxial thicknesses. The fitting coefficient of 0.91 yielded the best fit for the present device. We double-checked the value using an intersectional scanning electron microscopic image, and a factor of 0.90 was obtained, indicating reasonable agreement with the fitting coefficient. The difference of $\sim 10\%$ between the designed and actual thicknesses is ascribed to the distribution of the source elemental atomic/molecular beams in the MBE growth, meaning that the density of the atoms/molecules is relatively low at the edge of the wafer. In the present case, the device chip was taken from the edge of the 2 in. wafer, causing the difference in the thickness.

The calculated absorption spectra for each layer, including the absorbance in the rear Au-metal region, are presented in Fig. 3. The total absorbance obtained by summing all the absorption spectra is also shown (pink line). The fitting result well represents the measured absorbance of the thin-film device, excluding the 5–10% difference in the short-wavelength (<700 nm) and below-bandgap ($>1,100$ nm) region. These differences are mainly attributed to the contribution of the front metal grids to the reflection and the parasitic absorption loss induced by the Au back mirror. The simulated absorptions in the n-GaAs, i-GaInNAsSb, and p-GaAs layers, which contribute to the photocarrier generation in the device, are summed. As shown in Fig. 4, the summed absorbance (pink line) corresponds to the measured EQE spectrum (black line) reasonably well. This indicates that almost all the photocarriers generated inside the n-i-p layers were collected before recombination. On the other hand, comparison between Figs. 3 and 4 reveals that a large absorption loss occurs at the front n⁺-GaAs contact layer. This can be reduced by removing the n⁺-GaAs layer. However, for the multijunction structure, the loss is negligible, as most photons in the wavelength range of <870 nm are absorbed in the GaAs subcell before reaching the GaInNAsSb layer.

For applying the present light-confinement structure to MJSCs, we calculated the optimum designs of GaInP (1.8 eV)/GaAs (1.4 eV)/GaInNAsSb (1.1 eV) structures. The simulation was based on the transfer-matrix method, and the thicknesses of the subcells were optimized to balance each subcell current. Here, we assume that 100% of the absorbed photons are collected, which is the same situation for the present devices. According to the SHARP 37.9% triple-junction cell whose J_{SC} was 14.27 mA/cm² under an air mass- (AM-) 1.5 solar spectrum,^{26,27)} we adopted a J_{SC} goal of 13–14 mA/cm². To minimize the reflection loss, we consider the ARC comprising the SiO₂/SiN_x/TiO₂ triple

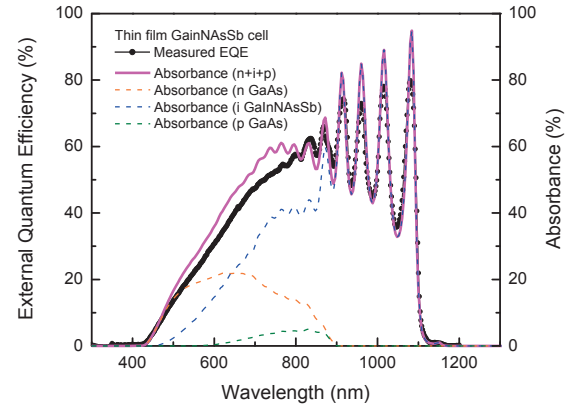


Fig. 4. Measured EQE and calculated absorption spectra of the n-i-p junction layers for the ELO thin-film GaInNAsSb cell.

Table III. Summary of the thicknesses for the TC, MC, and BC inputs to the calculation and the subcell J_{SC} values under AM-1.5 situation.

	Thicknesses (μm)			J_{SC} values (mA/cm^2)		
	Top	Middle	Bottom	Top	Middle	Bottom
Structure A	0.48	1.15	4.00	13.04	12.97	13.07
Structure B	0.48	1.15	2.00	13.04	12.98	13.01
Structure C	0.42	0.88	1.00	12.53	12.50	12.49
Structure D	0.72	2.70	1.00	14.22	14.23	14.22

layer in the calculation. Table III presents the thicknesses of each subcell and the calculated AM-1.5 J_{SC} values. For the non-transferred case (structure A), a thick bottom-cell (BC) absorber is needed to generate a photocurrent as high as 13 mA/cm², as the light-confinement effect confers no benefit. Hence, the GaInNAsSb BC thickness became 4.0 μm through the optimization, whereas the thicknesses of the top cell (TC) and middle cell (MC) were determined to be 0.48 and 1.15 μm , respectively. These values are smaller than those for the generally reported designs²⁸⁾ giving optimal performance. However, by sharing the photons transmitted through the upper subcells with lower subcells, as shown in Fig. 5(a), the proposed structure can balance the current generation among subcells, and a maximum J_{SC} of 13.0 mA/cm² can be obtained. On the other hand, if the device layer is transferred onto the reflector (structure B), the thickness of the GaInNAsSb BC can be reduced by half while the J_{SC} is maintained, because the OPL in the BC can be doubled by the effect of the back reflector. If there is no reflection of the incident light at the top of the device (i.e., with ideal ARC), the light not absorbed by the BC can travel only on a round trip, owing to the back reflector, and at the TC/air interface, the light escapes because no reflection occurs under this assumption. In this case, it might not be appropriate to label the phenomenon as light confinement; rather a light-trapping effect leads to an increase of the OPL twice. However, in the simulated situations, a more realistic ARC is assumed, and slight FP resonance features appear for the transferred structures, resulting from a small reflection at the top surface. It is a strong merit that the BC thickness can be reduced, because the GaInNAsSb cell needs the field-assisted carrier-collection process, and hence a thin i-region is preferable. However, a further decrease in the GaInNAsSb thickness to 1.0 μm (structure C) results in a lower J_{SC} value of

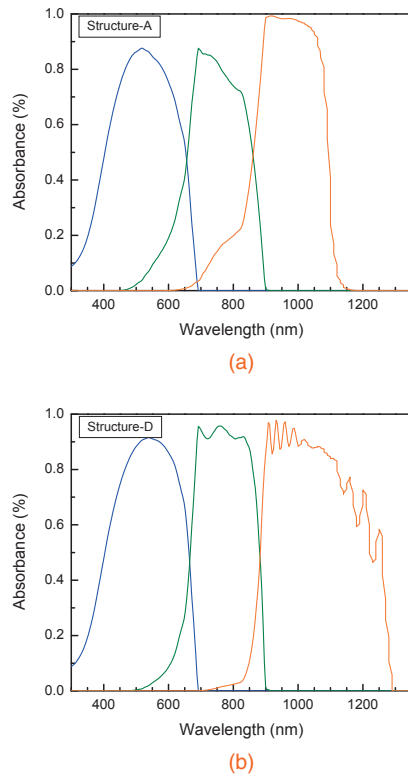


Fig. 5. Calculated subcell absorbance spectra of GaInP/GaAs/GaInNAsSb triple-junction solar cells with (a) structure A and (b) structure D.

$\sim 12.5 \text{ mA/cm}^2$, in spite of optimizing the TC and MC thicknesses. Considering terrestrial photovoltaic applications, the absorption bands due to the atmosphere around 900–990 and 1,070–1,170 nm restrict the photocurrent generation in the BC wavelength range. According to our calculation, in the case of a 1.1-eV GaInNAsSb BC beneath the 1.15- μm -thick GaAs MC, although 13 mA/cm^2 is obtained with an OPL of $4.0 \mu\text{m}$, an OPL of $>10 \mu\text{m}$ is needed to obtain 14 mA/cm^2 . Furthermore, because the TC and MC thicknesses were reduced in this calculation, the redesign of the TC and MC bandgap energies, as well as the thicknesses, is necessary so that the output current is not limited by these upper sub-cells. Otherwise, to generate a higher current in the BC, extending the absorption edge of the GaInNAsSb below 1,200 nm is more reasonable, which can be achieved with N and In compositions of >2 and $>6\%$, respectively. In the structure D, the BC bandgap of 1.0 eV was assumed, while the thickness was kept as $1.0 \mu\text{m}$. In this case, we can accept thick TC and MC structures, which have thicknesses comparable to those generally used, and a J_{SC} of 14.2 mA/cm^2 can be obtained.

In summary, we applied the W-ELO method to a dilute-nitride GaInNAsSb cell and characterized its solar-cell performance. The GaInNAsSb device thin film was successfully separated from its substrate without any cracks. In the present ELO thin-film cell, a clear FP resonance feature was observed, which is ascribed to the light-confinement effect. Compared with a reference GaInNAsSb cell having a rigid GaAs substrate, in the ELO thin-film cell, the light-confinement effect contributed to an enhancement of photocurrent. This brings merits in dilute-nitride solar cells, which have a poor minority-carrier lifetime and diffusion length, because

the maximum current can be achieved with a limited thickness of the absorber layer. Moreover, if the rear textured light-scattering pattern is utilized^{10,11)} instead of the presented flat mirror, a further increase in the OPL can be expected. By employing the dilute-nitride cell with light management for multijunction structures, through the ELO technique, it will be possible to realize low-cost MJSCs with a high yield and high conversion efficiencies.

Acknowledgments This work was supported by the Incorporated Administrative Agency New Energy and Industrial Technology Development Organization (NEDO) and the Ministry of Economy, Trade and Industry (METI), Japan. A part of this work was supported by JSPS KAKENHI Grant Number 16K21007.

- 1) M. Konagai, M. Sugimoto, and K. Takahashi, *J. Cryst. Growth* **45**, 277 (1978).
- 2) E. Yablonovitch, T. Gmitter, J. P. Harbison, and R. Bhat, *Appl. Phys. Lett.* **51**, 2222 (1987).
- 3) J. J. Schermer, G. J. Bauhuis, P. Mulder, W. J. Meulemeesters, E. Haverkamp, M. M. A. J. Voncken, and P. K. Larsen, *Appl. Phys. Lett.* **76**, 2131 (2000).
- 4) M. M. A. J. Voncken, J. J. Schermer, G. J. Bauhuis, P. Mulder, and P. K. Larsen, *Appl. Phys. A* **79**, 1801 (2004).
- 5) J. Adams, V. Elarde, A. Hains, C. Stender, F. Tuminello, C. Youtsey, A. Wibowo, and M. Osowski, *IEEE J. Photovoltaics* **3**, 899 (2013).
- 6) G. J. Bauhuis, P. Mulder, E. J. Haverkamp, J. J. Schermer, E. Bongers, G. Oomen, W. Köstler, and G. Strobl, *Prog. Photovoltaics* **18**, 155 (2010).
- 7) B. M. Kayes, H. Nie, R. Twist, S. G. Spruytte, F. Reinhardt, I. C. Kizilyalli, and G. S. Hignashi, *Proc. 37th IEEE Photovoltaic Specialists Conf. (PVSC)*, 2011, p. 000004.
- 8) R. Tatavarti, A. Wibowo, G. Martin, F. Tuminello, C. Youtsey, G. Hillier, N. Pan, M. W. Wanlass, and M. Romero, *Proc. 35th IEEE Photovoltaic Specialists Conf. (PVSC)*, 2010, p. 002125.
- 9) M. A. Steiner, J. F. Geisz, I. García, D. J. Friedman, A. Duda, and S. R. Kurtz, *J. Appl. Phys.* **113**, 123109 (2013).
- 10) K. Watanabe, B. Kim, T. Inoue, H. Sodabanlu, M. Sugiyama, M. Goto, S. Hayashi, K. Miyano, and Y. Nakano, *IEEE J. Photovoltaics* **4**, 1086 (2014).
- 11) K. Watanabe, T. Inoue, K. Toprasertpong, A. Delamarre, H. Sodabanlu, J.-F. Guillemoles, M. Sugiyama, and Y. Nakano, *Proc. 43rd IEEE Photovoltaic Specialists Conf. (PVSC)*, 2016, p. 1268.
- 12) B. Behaghel, R. Tamaki, N. Vandamme, K. Watanabe, C. Dupuis, N. Bardou, H. Sodabanlu, A. Cattoni, Y. Okada, M. Sugiyama, S. Collin, and J. F. Guillemoles, *Appl. Phys. Lett.* **106**, 081107 (2015).
- 13) K. W. J. Barnham, I. Ballard, J. P. Connolly, N. J. Ekins-Daukes, B. G. Kluffinger, J. Nelson, and C. Rohr, *Physica E* **14**, 27 (2002).
- 14) Y. Okada and N. Shiotsuka, *Proc. 31st IEEE Photovoltaic Specialists Conf. (PVSC)*, 2005, p. 591.
- 15) T. Nakata, K. Watanabe, N. Miyashita, H. Sodabanlu, M. Giteau, Y. Nakano, Y. Okada, and M. Sugiyama, submitted.
- 16) Y. Okada, N. Kobayashi, and N. Sasaki, *Proc. IEEE 4th World Conf. Photovoltaic Energy Conversion (WCPEC)*, 2006, p. 865.
- 17) R. Oshima, T. Hashimoto, H. Shigekawa, and Y. Okada, *J. Appl. Phys.* **100**, 083110 (2006).
- 18) Q. Xie, A. Madhukar, P. Chen, and N. P. Kobayashi, *Phys. Rev. Lett.* **75**, 2542 (1995).
- 19) T. Sogabe, Y. Shoji, P. Mulder, J. Schermer, E. Tamayo, and Y. Okada, *Appl. Phys. Lett.* **105**, 113904 (2014).
- 20) D. J. Friedman, J. F. Geisz, S. R. Kurtz, and J. M. Olson, *J. Cryst. Growth* **195**, 409 (1998).
- 21) S. R. Kurtz, A. A. Allerman, E. D. Jones, J. M. Gee, J. J. Banas, and B. E. Hammons, *Appl. Phys. Lett.* **74**, 729 (1999).
- 22) N. Miyashita, N. Ahsan, and Y. Okada, *Prog. Photovoltaics* **18**, 155 (2010).
- 23) C. W. Greeff and H. R. Glyde, *Phys. Rev. B* **51**, 1778 (1995).
- 24) M. K. Weilmeier, K. M. Colbow, T. Tiedje, T. V. Buren, and L. Xu, *Can. J. Phys.* **69**, 422 (1991).
- 25) S. L. Tan, C. J. Hunter, S. Zhang, L. J. J. Tan, Y. L. Goh, J. S. Ng, I. P. Marko, S. J. Sweeney, A. R. Adams, J. Allam, and J. P. R. David, *J. Electron. Mater.* **41**, 3393 (2012).
- 26) T. Takamoto, H. Washio, and H. Juso, *Proc. 40th IEEE Photovoltaic Specialists Conf. (PVSC)*, 2014, p. 0001.
- 27) M. A. Green, K. Emery, Y. Hishikawa, W. Warta, and E. D. Dunlop, *Prog. Photovoltaics* **21**, 827 (2013).
- 28) T. Takamoto, E. Ikeda, and M. Ohmori, *Appl. Phys. Lett.* **70**, 381 (1997).